REGULAR ARTICLE



Electrophysical Properties of [Ni₈₀Fe₂₀/SiO_x)]_n Discontinuous Multilayers

O.V. Pylypenko, I.M. Pazukha* [™] , S.R. Dolhov-Hordiichuck, A.M. Lohvynov, K.V. Tyschenko, D.S. Kabyletskyi, Yu.O. Shkurdoda¹

Sumy State University, 40007 Sumy, Ukraine

(Received 25 August 2025; revised manuscript received 18 October 2025; published online 30 October 2025)

In this research, [Ni₈₀Fe₂₀(d)/SiO_x(5)]₅/S discontinuous multilayers were fabricated using the method of layer-bylayer electron-beam evaporation. The phase composition, structural features, and electrophysical properties of the samples were investigated depending on the effective thickness of the ferromagnetic Ni₈₀Fe₂₀ layers and annealing temperature. Based on transmission electron microscopy and electron diffraction analysis, it was established that the samples exhibit a nanocrystalline structure of NisoFe20 grains embedded in an amorphous SiOx matrix, with a phase composition corresponding to fcc-Ni₃Fe, which remains stable after annealing at 500 and 700 K. The average grain size of $N_{180}Fe_{20}$ increases with thickness and annealing temperature, contributing to changes in transport properties. The temperature dependences of resistivity and the temperature coefficient of resistance (TCR) were studied within several heating/cooling cycles up to 600 K. It was found that for structures with Ni₈₀Fe₂₀ thickness d = 4 - 8 nm, a metallic conduction regime is realized, characterized by positive TCR values. In contrast, structures with d=3 nm demonstrate nearly constant resistivity with temperature and TCR values close to zero, indicating a transition conduction regime where metallic and tunneling mechanisms coexist. The annealing process leads to a reduction in resistivity due to structural ordering. The results confirm that both resistivity and TCR are monotonic functions of Ni₈₀Fe₂₀ layer thickness, which is associated with changes in grain size and intergranular distances. These findings are essential for tailoring the transport behavior of magnetic discontinuous multilayers for future applications in spintronics, sensors, and functional nanomaterials.

Keywords: Discontinuous thin-film systems, Permalloy, Annealing, Resistivity, Temperature coefficient of resistance.

DOI: 10.21272/jnep.17(5).05004 PACS numbers: 68.37. - d, 73.61. - r, 81.40.Ef

1. INTRODUCTION

In modern electronics, improving device performance while simultaneously minimising size and energy consumption remains a key challenge. Metal-insulator nanocomposites, those composed of ferromagnetic metal Fe, Co, Ni or their alloys Ni_xFe_{1-x}, Fe_xCo_{1-x} and insulators like SiO₂, HfO₂, MgO, etc., have garnered significant attention due to their promising magnetic, magnetooptical, magnetoresistive, and electrical properties [1-5]. The precise control of the size and arrangement of metallic nanoparticles in an insulator matrix results in precise control of their properties. They can display a range of phenomena such as giant magnetoresistance (GMR) [6], the Hall effect [7], Kerr magnetooptical effect [8], and memristive effect [9]. This offers their potential applications in various fields, including microelectronics, sensor technologies, and optics [10-12]. At the same time, the electrophysical properties of ferromagnetic metalinsulator composite materials, which differ significantly from the properties of bulk metal samples and continuous homogeneous films, are also important [13-15].

Ferromagnetic metal-insulator FM represents a special type of nanostructure/I discontinuous multilayers (DMIM), which feature a transition from the two-dimensional continuous to the discontinuous three-dimensional case. Different structures, ranging from insulation to metallic, can be obtained by varying the nominal thickness of the ferromagnetic and insulator layers [16, 17].

In this work, we studied the $[Ni_{80}Fe_{20}/SiO_x]_n/S$ discontinuous multilayers to reveal the influence of the effective thickness of ferromagnetic layers on their electrophysical properties (the value of resistivity and temperature coefficient of resistance).

2. EXPERIMENTAL DETAIL

The $[Ni_{80}Fe_{20}(d)/SiO_x(5)]_5/S$ discontinuous multilayers, where $x \cong 1$, were prepared at room temperature (RT) in a vacuum chamber with a base pressure of 10^{-4} Pa. The method of layer-by-layer electron-beam evaporation was used for the deposition of samples. The thickness of the

2077-6772/2025/17(5)05004(5)

05004-1

https://jnep.sumdu.edu.ua

© 2025 The Author(s). Journal of Nano- and Electronics Physics published by Sumy State University. This article is distributed under the terms and conditions of the Creative Commons Attribution (CC BY) license.

^{*} Correspondence e-mail: i.pazuha@aph.sumdu.edu.ua

magnetic layers (d) varied from 3 to 8 nm. The thickness of the layers was controlled by two independent in situ quartz resonators with an accuracy of 10%.

The annealing was performed in a vacuum chamber at 10^{-4} Pa. For the research of electrophysical properties, the samples after deposition were annealed during several cycles of "heating \leftrightarrow cooling" up to the annealing temperature $(T_{\rm ann})$ of 400, 500, and 600 K. The measurement of resistivity is carried out in current inplane geometry. The value of the temperature coefficient of resistance (TCR) has been calculated based on the temperature dependences of resistance by the equation: $\beta = (1/R_{\rm in}) (\Delta R/\Delta T)$, where $R_{\rm in}$ is the initial value of resistance, $\Delta T = T_{\rm ann} - {\rm RT}$.

Transmission electron microscopy (TEM-125K) has been used to investigate the crystalline structures of the samples.

3. RESULTS AND DISCUSSION

For correct interpretation of the electrophysical properties of [Ni₈₀Fe₂₀(*d*)/SiO_x(5)]₅/S discontinuous multilayer, the peculiarities of their phase state and crystal structure under annealing were first studied. Fig. 1 displays

the diffraction patterns for $[Ni_{80}Fe_{20}(4)/SiO_x(5)]_5/S$ discontinuous multilayers after deposition and annealing at temperatures of 500 and 700 K. The analysis demonstrates that the phase state of the sample after deposition (Fig. 1a) corresponds to the fcc- Ni_3Fe structure [18]. The insulator is amorphous [19], and indexing reflections corresponding to SiO_x is impossible. The phase state does not change after samples are annealed at a temperature of 500 K (Fig. 1b) and 700 K (Fig. 1c). The formation of oxide phases after annealing at 500 and 700 K was not fixed electronographically. The lattice parameter of the fcc- Ni_3Fe structure slightly grows under annealing from 0.355 nm to 0.358 nm.

The results of bright-film TEM images (Fig. 2) studies allow us to conclude that the $[Ni_{80}Fe_{20}(d)/SiO_x(5)]_5/S$ discontinuous multilayers with the effective thickness of $Ni_{80}Fe_{20}$ layers of 8 nm (Fig. 2a) and 4 nm (Fig. 2d) are nanocrystalline in the as-deposited state. Notably, the structure of the samples is typical for nano-granular films (see, for example, [2, 15]), namely, $Ni_{80}Fe_{20}$ grains are embedded in the insulating SiO_x matrix. The average size of $Ni_{80}Fe_{20}$ grains is 8-12 nm at d=8 nm and decreases to 4-7 nm when d=4 nm.

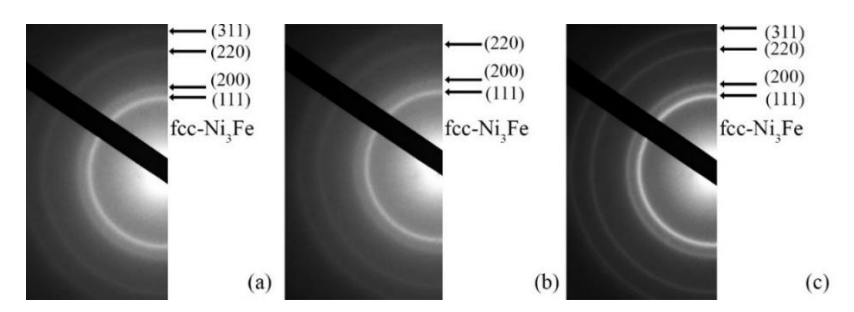


Fig. 1 – Diffraction patterns for [NisoFe20(4)/SiOx(5)]s/S discontinuous multilayers after deposition (a) and annealing at 500 (b) and 700 K (c)

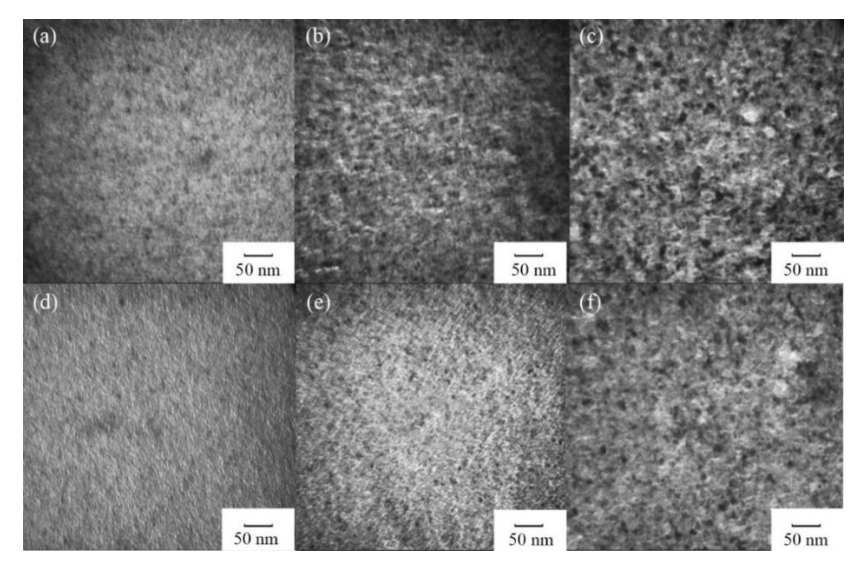


Fig. 2 – TEM images for $[Ni_{80}Fe_{20}(d)/SiO_x(5)]_5/S$ discontinuous multilayers with the effective thickness of $Ni_{80}Fe_{20}$ layers d=8 nm (a-c) and 4 nm (d-f) after deposition (a, B) and annealing at 500 K (b, e) and 700 K (c, f)

Besides, for $[Ni_{80}Fe_{20}(8)/SiO_x(5)]_5/S$ discontinuous multilayers, some $Ni_{80}Fe_{20}$ grains form interconnected clusters, creating a heterogeneous microstructure with coexisting isolated $Ni_{80}Fe_{20}$ grains and $Ni_{80}Fe_{20}$ clustered configurations [5]. So, at the effective thickness of $Ni_{80}Fe_{20}$ layers d=8 nm, the metal layers can be "electrically continuous" due to the formation of ferromagnetic clusters. Substantial structural changes are observed only after annealing at 700 K (Fig. 2c, 2f). All samples' average $Ni_{80}Fe_{20}$ grain size grew by 1,5-2 times.

To establish the mechanisms of conductivity in the $[Ni_{80}Fe_{20}(d)/SiO_x(5)]_5/S$ discontinuous multilayers, the temperature dependence of resistivity was obtained. Fig. 3 shows the $\rho(T)$ dependence within the 300-600 K range for systems with different effective thicknesses of metal layers $Ni_{80}Fe_{20}$. For structures with d = 4-8 nm, the growth of the resistivity value with increasing annealing temperature is realised. In this case, the electron transport processes in these discontinuous multilayers are caused by conduction through metal clusters formed and determined by the scattering of conduction electrons at grain boundaries, impurities and phonons. For structures with d = 3 nm, the resistivity value remains practically unchanged with increasing temperature to 600 K. This corresponds to the conductivity transition regime. In the transition regime. conductivity is a superposition of two mechanisms: metallic conduction in large metal clusters and tunnelling between individual metal clusters separated by a thin insulator layer.

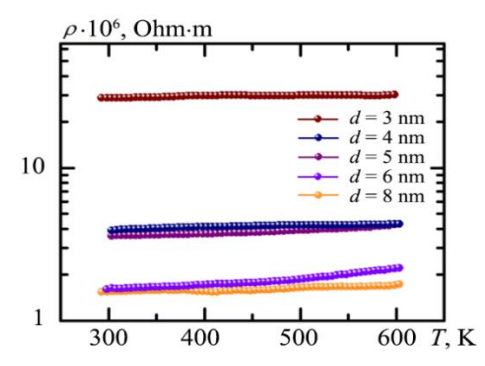


Fig. 3 – Temperature dependences of resistivity for $[Ni_{80}Fe_{20}(d)/SiO_x(5)]_5/S$ discontinuous multilayers at the effective thickness of $Ni_{80}Fe_{20}$ layer d=3-8 nm

Fig. 4 illustrates the evolution of the resistivity and TCR values after gradual annealing at the temperatures of 400, 500, and 600 K, with the different effective thicknesses of the Ni $_{80}$ Fe $_{20}$. Annealing the samples at 400, 500 and 600 K leads to an irreversible decrease in resistivity regardless of d (Fig. 4a). This is due to improvements in the crystal structure of the metal layers, i.e. the healing of crystal structure defects.

Based on experimental data of resistance during cooling, the calculation of the temperature coefficient of resistance was done (Fig. 4b). Since for samples with d=4-8 nm, the metallic mode of conductivity is observed, the temperature coefficient of resistance has a positive value.

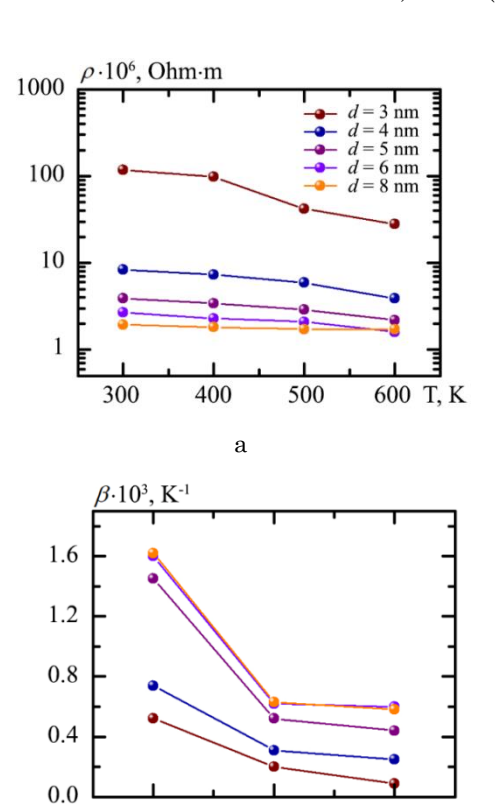


Fig. 4 – Resistivity (a) and temperature coefficient of resistance (b) as a function of annealing temperature for $[Nis_0Fe_{20}(d)/SiO_x(5)]_5/S$ discontinuous multilayers with the effective thickness of Nis_0Fe_{20} layers d=3-8 nm

b

500

T, K

600

400

Note that for samples with d=3 nm, annealing at a temperature of 600 K leads to almost zero TCR values. The values of TCR are close to zero due to the implementation of the transition conduction regime. The condition TCR = 0 is fulfilled for such volume fractions of the metal phase and at such temperatures when the contributions from the metal conductivity of clusters and tunnelling are equal.

Consider the peculiarities of the dependence of resistivity on the effective thickness of the ferromagnetic layer d (Fig. 5a). As can be seen from Fig. 5a, the resistivity of both as-deposited samples and annealed at 400, 500, and 600 K monotonically decreases with increasing effective thickness of the Ni₈₀Fe₂₀ layers. The maximum resistivity value is observed for as-deposited structures with a minimum thickness of Ni₈₀Fe₂₀ layers (d = 3 nm) and is $118 \cdot 10^{-6} \text{ Ohm-m}$. With an effective thickness of Ni₈₀Fe₂₀ layers d = 8 nm, the resistivity reaches its minimum value, which for samples annealed at a temperature of 600 K is 0.89·10⁻⁶ Ohm m. Relatively large resistivity values, even for samples annealed at 600 K, can be explained by the fact that the metal layers are in a nanocrystalline state. This leads to an increased influence of conduction electron scattering on defects and grain boundaries [20, 21].

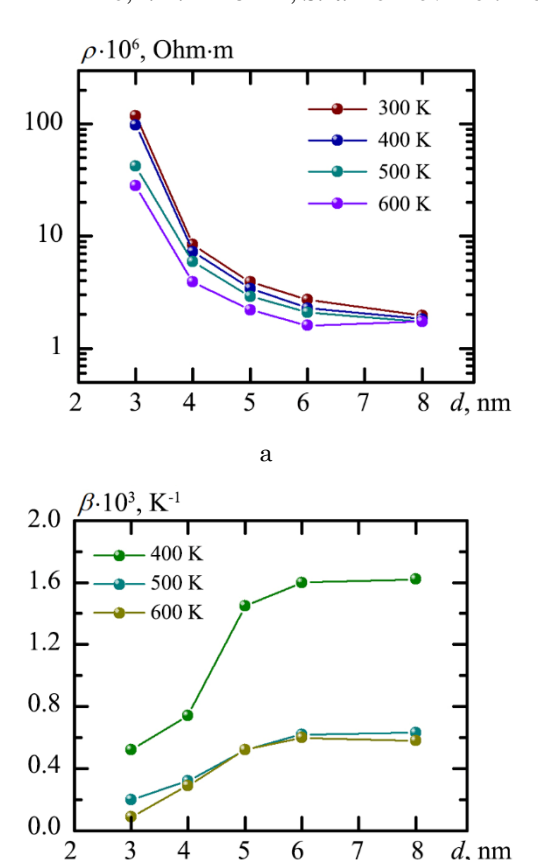


Fig. 5 - Resistivity (a) and temperature coefficient of resistance (b) as a function of the effective thickness of $Ni_{80}Fe_{20}$ layer d for [Ni₈₀Fe₂₀(d)/SiO_x(5)]₅/S discontinuous multilayers

b

d, nm

The temperature coefficient of resistance as a function of the effective thickness of Ni₈₀Fe₂₀ layer d for $[Ni_{80}Fe_{20}(d)/SiO_x(5)]_5/S$ discontinuous multilayers is shown in Fig. 5b. All dependences of $\beta(d)$ are monotonic. The value of the TCR increases with the increase in the effective thickness of the Ni₈₀Fe₂₀ layers. This size dependence is due to the influence of effective thickness on

the evolution of the size distribution of metal granules. Thus, neglecting any chemical interaction between the granules and the matrix, increasing the effective thickness of the metal layers generally has two effects on the evolution of the grain size distribution: increasing the average metal grain size (increasing the grain density) and decreasing the distance between them.

CONCLUSION

The structural and electrophysical properties of the $[Ni_{80}Fe_{20}(d)/SiO_{x}(5)]_{5}/S$ discontinuous multilavers prepared by the method of layer-by-layer electron-beam evaporation have been studied as a function of the effective thickness of Ni₈₀Fe₂₀ layers. From the diffraction patterns analysis, we conclude that the phase state of the samples after deposition and annealing at a temperature of 500 and 700 K correspond to the fcc-Ni₃Fe structure. Their microstructure consists of interconnected ferromagnetic grains embedded within an amorphous SiO_x matrix. It is established that the resistivity's size dependence and the resistance's temperature coefficient are monotonic in nature. The resistivity value decreases, and the TCR increases with the effective thickness of Ni₈₀Fe₂₀ layers. It was demonstrated that at d = 4-8 nm, the metallic regime of conductivity, determined by the conductivity through the disordered metal matrix, with positive values of TCR, is observed. At the effective thickness of Ni₈₀Fe₂₀ of 3 nm, the transition mode of conductivity with close to zero TCR is observed. In the transition regime, conductivity is a superposition of two mechanisms: metallic conduction in large metal clusters and tunnelling between individual metal clusters separated by a thin insulator layer.

ACKNOWLEDGMENTS

This work was funded by the NATO Program "Science for Peace and Security" (project number G6131) and the State Program of the Ministry of Education and Science of Ukraine (project number 0224U033036 0124U003644).

REFERENCES

- 1. I. Suzuki, T. Abe, H. Sepehri-Amin, K. Hono, Y.K. Takahashi, J. Magn. Magn. Mater. **579**, 170874 (2023).
- I.M. Pazukha, V.V. Shchotkin, Yu.O. Shkurdoda, Prog. Phys. Met. 20, No 4, 672 (2019).
- A. Wilczy'nska, T.N. Kołtunowicz, A. Kociubi'nski, B. Guzowski, M. Łakomski, J. Magn. Magn. Mater. 597, 172030 (2024).
- 4. C. Wang, Y. Zhang, P. Zhang, Y. Rong, T.Y. Hsu, J. Magn. Magn. Mater. 320, 683 (2008).
- Y. Zou, L. Wang, B. Fan, J. Yue, Yu Liu, X. Huang, Appl. Surf. Sci. 699, 163124 (2025).
- A. Milner, A. Gerber, B. Groisman, M. Karpovsky, A. Gladkikh, Phys. Rev. Lett. 76, 475 (1996).
- J. Sonntag, *J. Compos. Mater.* **6**, 78 (2016).
- F. Royer, B. Vargehese, E. Gamet, S. Nebeu, Y. Jourlin, D.

- Jamon, ACS Omega 5, No 6, 2886 (2020).
- H. Silva, H.L. Gomes, Yu.G. Pogorelov, P. Stallinga, D.M. de Leeuw, J.P. Araujo, J.B. Sousa, S.C.J. Meskers, G. Kakazei, S. Cardoso, P.P. Freitas, Appl. Phys. Lett. 94, 202107 (2009).
- 10. A. Ashery, G. Khabiri, A. Hassan, M.M.K. Yousef, A.S.G Khalil, Mater. Sci. Semicond. Proc. 104, 104652 (2019).
- 11. M. Nichterwitz, S. Honnali, J. Zehner, S. Schneider, D. Pohl, S. Schiemenz, S.T.B. Goennenwein, K. Nielsch, K. Leistner, ACS Appl. Electron. Mater. 2, 2543 (2020).
- 12. S.E. Rannala, A. Meo, S. Ruta, W. Pantasri, R.W. Chantrell, P. Chureemart, J. Chureemart, Comp. Phys. Commun. 279, 108462 (2022).
- 13. M.A.S. Boff, B. Canto, F. Mesquita, R. Hinrichs, G.L.F. Fraga, L.G. Pereira, J. Appl. Phys. 120, 155103 (2016).
- 14. A. Chornous, I. Protsenko, I. Shpetnyi, Cryst. Res. Technol.

- **39**, 602 (2004)
- X. Li, Y. Li, Y. Shia, F. Du, Y. Bai, Z. Quan, X. Xu, *Mater. Lett.* 194, 227 (2017).
- I.M. Pazukha, A.M. Lohvynov, K.V. Tyschenko,
 O.V. Pylypenko, Yu.O. Shkurdoda, V. Komanicky, MRS Commun. 14, 56 (2024).
- 17. R. Brucas, M. Hanson, J. Magn. Magn. Mater. 310, 2521 (2007).
- 18. L. Taberkani, A. Kharmouche, *Phys. B* **656**, 414782 (2023).
- A. Hirata, S. Kohara, T. Asada, M. Arao, C. Yogi, H. Imai,
 Y. Tan, T. Fujita, M. Chen, *Nature Commun.* 7, 11591 (2016).
- A.B. Rinkevich, D.V. Perov, V.O. Vaskovsky,
 A.N. Gorkovenko, E.A. Kuznetsov, IEEE Transac.
 Nanotechnol. 16, 1067 (2017).
- M. Anas, C. Bellouard, L. Moreau, M. Vergnat, J. Magn. Magn. Mater. 284, 165 (2004).

Електрофізичні властивості шаруватих структур $[Ni_{80}Fe_{20}/SiO_x)]_n$

О.В. Пилипенко, І.М. Пазуха, С.Р. Долгов-Гордійчук, А.М. Логвинов, К.В. Тищенко, Д.С. Кабилецький, Ю.О. Шкурдода

Сумський державний університет, 40007 Суми, Україна

У даній роботі за допомогою методу пошарового електронно-променевого випарювання було виготовлено серію шаруватих структур $[Ni_{80}Fe_{20}(d)/SiO_x(5)]_5/\Pi$ з різною ефективною товщиною феромагнітних шарів Ni₈₀Fe₂₀. Досліджено фазовий склад, мікроструктуру та електрофізичні властивості зразків залежно від товщини металевих шарів та температури відпалу. За результатами електронної дифракції та трансмісійної електронної мікроскопії встановлено, що зразки мають нанокристалічну структуру, де зерна Ni80Fe20 впроваджені в аморфну матрицю SiO_x, а їх фазовий стан відповідає структурі ГЦК-Nі₃Fe і зберігається навіть після відпалу при 500 і 700 К. Середній розмір зерен зростає зі збільшенням товщини шару та температури відпалу, що зумовлює зміни в транспортних характеристиках. Температурні залежності питомого опору та температурного коефіцієнта опору (ТКО) досліджено в межах декількох циклів «нагрівання \leftrightarrow охолодження» до 600 К. Виявлено, що для структур з товщиною $Ni_{80}Fe_{20}$ d=4-8 нм реалізується металевий режим провідності, що характеризується додатними значеннями ТКО. Натомість при d=3 нм питомий опір практично не змінюється з температурою, а ТКО наближається до нуля, що вказує на реалізацію перехідного режиму провідності зі спільною дією металевої та тунельної провідності. Встановлено, що процес відпалу сприяє зниженню питомого опору за рахунок покращення кристалічної структури. Результати демонструють монотонний характер залежностей питомого опору та ТКО від товщини шарів Ni₈₀Fe₂₀, що зумовлено еволюцією розмірів зерен та міжзеренних відстаней. Отримані дані є перспективними для цілеспрямованого керування провідністю у феромагнітних багатошарових структурах для застосування у спінтроніці, сенсориці та функціональних наноматеріалах.

Ключові слова: Шаруваті тонкоплівкові системи, Пермаллой, Відпалювання, Питомий опір, Температурний коефіцієнт опору.